Condensation of Methane, Ammonia, and Water and the Inhibition of Convection in Giant Planets

Author(s): Tristan Guillot

Source: *Science*, Sep. 22, 1995, New Series, Vol. 269, No. 5231 (Sep. 22, 1995), pp. 1697-1699

Published by: American Association for the Advancement of Science

Stable URL: http://www.jstor.com/stable/2888575

Condensation of Methane, Ammonia, and Water and the Inhibition of Convection in Giant Planets

Tristan Guillot

The condensation of chemical species of high molecular mass such as methane, ammonia, and water can inhibit convection in the hydrogen-helium atmospheres of the giant planets. Convection is inhibited in Uranus and Neptune when methane reaches an abundance of about 15 times the solar value and in Jupiter and Saturn if the abundance of water is more than about five times the solar value. The temperature gradient consequently becomes superadiabatic, which is observed in temperature profiles inferred from radio-occultation measurements. The planetary heat flux is then likely to be transported by another mechanism, possibly radiation in Uranus, or diffusive convection.

The visible appearance of the giant planets is dominated by the presence of ammonia clouds in Jupiter and Saturn and methane clouds in Uranus and Neptune. Condensation and consequent cloud formation affect the atmosphere's chemical composition (*1*) and spectral appearance (*2*). They also impact the nature of convection and, consequently, the internal structure of these planets. The transition from a vapor to a condensed phase releases latent heat and generally favors rapid upwellings (*3*, *4*). It can also inhibit convection because, contrary to the case of water in Earth's atmosphere, the mean molecular mass in the giant planets' atmospheres (mainly consisting of hydrogen and helium) is always smaller than that of the condensable species (*3*, *5*). Here, I examine this latter effect and its consequences for the transport properties of the atmosphere.

I consider a solution of two species, one uncondensable (of mass m_u and density ρ_u), whereas the other (mass m_v and density ρ_v) is present both in vapor and in a condensed phase (solid or liquid). I assume that the ideal gas equation of state applies and that the volume of the condensed phase can be neglected compared to the volume of the vapor phase. I also assume that the medium is saturated and that the condensed species are instantaneously removed by sedimentation (*6*).

The gradient of mean molecular weight μ in the atmosphere is obtained directly from the Clausius-Clapeyron equation

$$\nabla_\mu \equiv \frac{d(\ln \mu)}{d(\ln P)} = \varpi f(\beta \nabla_T - 1) \qquad (1)$$

where P is the pressure, $\nabla_T \equiv d(\ln T)/d(\ln P)$ is the temperature gradient in the atmosphere, $\beta = L/RT$ is the ratio of the latent heat of condensation L to the thermal energy RT (R is the gas constant), $f = \rho_u/\rho_v$ is the mass mixing ratio of the condensable species, and $\varpi = (1 - m_u/m_v)/(1 + f)$. Relevant conditions are characterized by $\beta \sim 20$, $\nabla_T \sim 0.3$, and $\varpi \sim 1$, so that $\nabla_\mu > 0$ always holds. This corresponds to the stabilizing case where the mean molecular weight increases with depth. In the case of terrestrial water clouds, $\varpi \sim -0.5$, and therefore, $\nabla_\mu < 0$.

A local criterion for convective instability can be determined by comparing the density of a (saturated) parcel of fluid arbitrarily lifted by a height dz to the density of the (saturated) environment (*7*). The compositional gradient in the environment, ∇_μ, is directly given by Eq. 1. The same equation also applies in the parcel, but the temperature gradient is ∇^*_{ad} [the moist pseudoadiabat (*8*)] instead of ∇_T. The instability criterion is then

$$(1 - \varpi\beta f)(\nabla_T - \nabla^*_{ad}) > 0 \qquad (2)$$

Because I assume that the medium would be convective in the absence of condensation, $\nabla_T > \nabla^*_{ad}$ (*9*).

Hence, convection is inhibited when the abundance of the condensable is such that

$$f > f_0 \equiv \frac{1}{\varpi\beta} \qquad (3)$$

Physically, this condition results from the fact that the abundance of condensable species drops faster in the environment than in the rising parcel. In spite of its higher temperature, the parcel thus becomes negatively buoyant. The values of f_0 for the condensation of methane, ammonia, and water in the four giant planets calculated with the use of Voyager radio-occultation measurements (*10*) and interior models (*11*) are given in Table 1. A relatively small enrichment of water or methane above the solar value is sufficient to inhibit convection. In particular, the values for methane in Uranus ($f_0 = 14.1$) and Neptune ($f_0 = 14.9$) are substantially lower than the abundances derived from spectroscopic measurements, which indicate enrichments between 30 and 60 times the solar value for both planets (*12*, *13*).

Table 1. Enrichment over solar value (*28*) above which convection is inhibited (assuming all C, N, and O atoms are used to form CH_4, NH_3, and H_2O, respectively). Note that CH_4 does not condense in Jupiter and Saturn.

Species	Jupiter	Saturn	Uranus	Neptune
CH_4	—	—	14.1	14.9
NH_3	32.6	33.5	53.6	57.1
H_2O	4.6	4.9	6.3	6.7

Equation 2 is calculated under the most favorable case for convection. If the condensed materials are not removed instantaneously by sedimentation or if the environment is not saturated, then any upwelling plume will also have to overcome a strongly stabilizing compositional gradient. On the other hand, a subsaturated plume will be able to rise through a saturated environment. This does not constitute an instability mechanism because it will rapidly transport all of the condensable species down until saturation is reached everywhere.

However, the atmosphere is still potentially unstable: A parcel that is forced to rise over a finite distance faster than it loses heat will eventually become buoyant, even though Eq. 3 is satisfied. This is a result of the local nature of this criterion. Nevertheless, the negative buoyancy that is associated with Eq. 3 is strong, and moist convection seems difficult to maintain in the region where $f > f_0$: For example, the possibility that moist convection could be forced by penetration from the bottom requires velocities much larger than typical convective velocities (Fig. 1).

If convection is inhibited, the tempera-

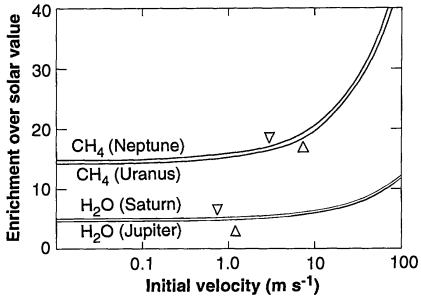

Fig. 1. Enrichment over solar value necessary to stop the progression of a saturated upwelling plume in a saturated environment for various initial velocities at the base of a water cloud in Jupiter and Saturn and a methane cloud in Uranus and Neptune. It is assumed that all the condensates fall rapidly and do not hinder the ascent of the plume. The enrichments found are equal to the values f_0 given in Table 1 in the limit of zero initial velocity. The triangles indicate typical values of the convective velocities in these regions [calculated with the use of mixing length theory and interior models from (*11*)].

Lunar and Planetary Laboratory, University of Arizona, Tucson, AZ 85721, USA.

ture gradient will increase until some mechanism becomes capable of transporting the heat flux. In any case, the superadiabaticity $\nabla_T - \nabla_{ad}$ (where ∇_{ad} is the dry adiabatic gradient) cannot grow much larger than the compositional gradient ∇_μ, above which the atmosphere becomes locally unstable to dry convection (*7*). However, other mechanisms, such as radiation or diffusive convection (*14*), may transport the heat flux with a smaller gradient. Neglecting the effects of condensation and compressibility, the criterion for diffusive convection to occur is given by oceanographic evidence (*15*), laboratory experiments (*16*), and theoretical arguments (*17, 18*)

$$\frac{D + \nu}{K + \nu} \nabla_\mu \leq \nabla_T - \nabla_{ad} \leq \nabla_\mu \qquad (4)$$

where K is the radiative diffusivity [calculated with Rosseland opacities from (*19*)], D is the microscopic diffusion coefficient of the condensable species, and ν is the kinematic viscosity. Except for huge abundances of condensed particles that are ruled out by observations of visible absorption in the methane cloud (or haze) of Uranus and Neptune (*20, 21*), K is always much larger than the thermal diffusivity. Hence, $K \gg \nu$ and $D \approx \nu$ at the levels where water condenses in Jupiter and Saturn and methane condenses in Uranus and Neptune, so that the overstability criterion (Eq. 4) is verified in these regions. Furthermore, because diffusive interfaces are then unstable to diffusive convection (*18*), layered convection is unlikely to occur, contrary to what is observed in Earth's oceans (*14, 15*) and suggested for Uranus (*22*). Diffusive convection then corresponds to weakly amplified oscillatory motions (with periods of the order of ≈10 min) and as such should dry out the atmosphere substantially below the saturation level.

Radio-occultation measurements of the four giant planets by Voyager 2 confirm some of these conclusions and provide some clues about the transport mechanisms in their atmospheres. As expected from Table 1 and the moderately small enrichments in ammonia observed in Jupiter and Saturn [~2 and ~2 to 4, respectively (*12*)], the condensation of this molecule has no noticeable effect on the temperature gradient, which becomes adiabatic near 0.8 bar (Fig. 2). In Uranus and Neptune, the region where methane condenses (and the associated compositional gradient ∇_μ is significant) is characterized by a temperature gradient that is much larger than the moist adiabat and significantly superadiabatic compared to the dry adiabat. This conclusion is independent of the assumed methane abundance used to retrieve the temperature profile from the occultation data (*23*). For temperatures lower than about 75 K ($P < 0.9$ bar in Uranus and $P < 1.2$ bars in Neptune), the observed gradient is consistent with a convective process obeying the Ledoux criterion (*7*). Deeper, diffusive convection probably limits the superadiabaticity to less than ∇_μ. Uranus's gradient is also consistent with a radiative transport of the heat flux, if 30% of the solar flux is absorbed above the 0.8-bar level of the atmosphere. Larger but strongly latitude-dependent absorption factors are measured (*20*) at slightly deeper levels (around 1.2 bars). This result would explain why CO is observed on Neptune and not on Uranus (*13, 24*).

Observations of the propagation of waves after the impact between the comet Shoemaker-Levy 9 and Jupiter (*25*) have been interpreted as gravity waves formed in the 20-bar region, where the abundance of water would be 10 times the solar value (*26*). An abundance of water only about 5 times the solar value [which is more consistent with the gravitational moments of this planet (*11*)] would lead to a large static stability and could possibly explain the observed wave speed. Thus, as observed in Uranus and Neptune, we expect the temperature gradient to become superadiabatic at levels where water condenses in Jupiter. The spacecraft Galileo will soon probe the jovian atmosphere down to the 20-bar level and tell us more about its structure. The study of convection in stratified planetary atmospheres will also help to understand the related phenomenon of semiconvection in stars (*7, 18*).

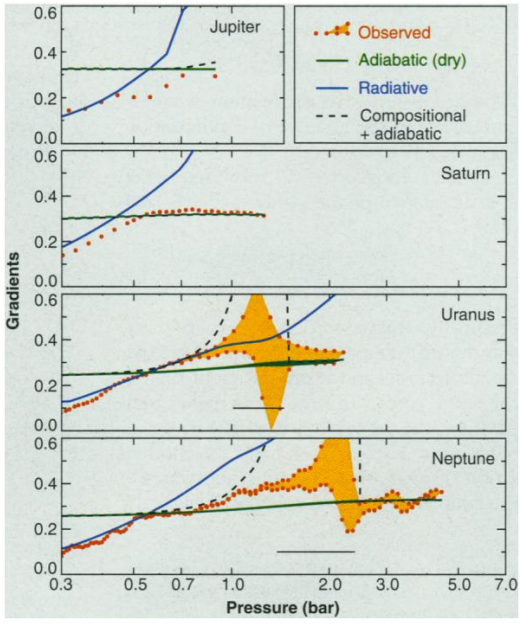

Fig. 2. Comparison of the atmospheric temperature gradient $\nabla_T \equiv d(\ln T)/d(\ln P)$ deduced from radio occultation measurements (*8, 9*) (red circles and filled areas) to the (equilibrium) dry adiabatic gradient ∇_{ad} (*27*) (green lines), the radiative gradient (blue lines), and the sum of the adiabatic and saturated compositional gradients $\nabla_{ad} + \nabla_\mu$ (black dashed lines). The black horizontal bars characterize regions where Eq. 3 is satisfied and $\nabla_\mu > 0$. In Uranus and Neptune, because of the large gradient of abundance of methane, one cannot retrieve both temperature profiles and methane abundances simultaneously from the data. Thus, plausible values for the temperature gradient are indicated by the filled areas (*23*). The radiative gradients are calculated within the diffusion approximation and assuming a luminosity equal to the sum of the internal and absorbed solar luminosities at all levels, except for Uranus and Neptune, where it is assumed that 30% of the solar heat flux has been absorbed at the 0.8-bar level. The moist adiabatic gradient ∇^*_{ad} is always inferior to the dry adiabatic gradient and is not represented here. Convection is not affected by the condensation of ammonia in Jupiter ($P \lesssim 0.9$ bar) and in Saturn ($P \lesssim 1.8$ bars). Water condenses at deeper levels that have not been observed. On the other hand, methane is very abundant in Uranus and Neptune and inhibits convection, as seen by the significant superadiabaticity in the 0.6- to 1.4-bar region in Uranus, and in the 1.0- to 2.3-bar region in Neptune. To obtain temperature lapse rates in kelvin per kilometer, multiply the gradients shown here by 6.8, 2.7, ~2.6, and ~3.5 for Jupiter, Saturn, Uranus, and Neptune, respectively.

REFERENCES AND NOTES

1. J. S. Lewis, *Icarus* **10**, 365 (1969).
2. A. Marten *et al.*, *ibid.* **46**, 233 (1981).
3. C. R. Stoker, *ibid.* **67**, 106 (1986); _____ and O. B. Toon, *Geophys. Res. Lett.* **16**, 929 (1989).
4. J. I. Lunine and D. M. Hunten, *Icarus* **69**, 566 (1987); *Planet. Space Sci.* **37**, 151 (1989); A. D. Del Genio and K. B. McGratten, *Icarus* **84**, 29 (1990); Y. Yair, Z. Levin, S. Tzivion, *ibid.* **98**, 72 (1992).
5. F. M. Flasar, paper presented at the Uranus Colloquium, 28 June to 1 July 1988, Pasadena, CA, see *Abstract Booklet JPL D-5504*, p. 3.8.
6. There is observational evidence that water in Jupiter [G. L. Bjoraker, H. P. Larson, V. G. Kunde, *Icarus* **66**, 579 (1986); B. E. Carlson, A. A. Lacis, W. B. Rossow, *Astrophys. J.* **388**, 648 (1992)] and methane in Uranus and Neptune (*10*) are significantly undersaturated. Moreover, the removal of condensed species is generally rapid compared to the Earth case [W. B. Rossow, *Icarus* **36**, 1 (1978); B. E. Carlson, W. B. Rossow, G. S. Orton, *J. Atmos. Res.* **45**, 2067 (1988)], but not enough for the presence of condensed material to be neglected in very strong upwellings (*3, 4*). Thus, I only consider here the most favorable case for convection.
7. P. Ledoux, *Astrophys. J.* **125**, 242 (1947); see also R. Kippenhahn and A. Weigert, *Stellar Structure and Evolution* (Springer-Verlag, Berlin, 1990).
8. K. A. Emanuel, *Atmospheric Convection* (Oxford Univ. Press, New York, 1994).
9. Except in the upper troposphere, the condition $\nabla_T < \nabla^*_{ad}$ would imply an unphysical heat transport from the top to the bottom of the atmosphere.
10. G. F. Lindal, D. N. Sweetnam, V. R. Eshleman, *As-*

tron. J. **90**, 1136 (1985); G. F. Lindal *et al.*, *J. Geophys. Res.* **92**, 14987 (1987); G. F. Lindal, *Astron. J.* **103**, 967 (1992).
11. T. Guillot, G. Chabrier, D. Gautier, P. Morel, *Icarus* **112**, 57 (1994).
12. D. Gautier and T. Owen, in *Origin and Evolution of Planetary and Satellite Atmospheres*, S. K. Atreya, J. B. Pollack, M. S. Matthews, Eds. (Univ. of Arizona Press, Tucson, 1989), pp. 487–512.
13. D. Gautier, B. J. Conrath, T. Owen, I. De Pater, S. K. Atreya, in *Neptune*, D. Cruikshank, Ed. (Univ. of Arizona Press, Tucson, in press).
14. J. S. Turner, *Buoyancy Effects in Fluids* (Cambridge Univ. Press, Cambridge, 1973); R. W. Schmitt, *Annu. Rev. Fluid Mech.* **26**, 255 (1994).
15. V. T. Neal, S. Neshyba, W. Denner, *Science* **166**, 373 (1969).
16. T. G. L. Shirtcliffe, *Nature* **213**, 489 (1967).
17. G. Veronis, *J. Fluid Mech.* **34**, 315 (1968).
18. D. J. Stevenson, *Mon. Not. R. Astron. Soc.* **187**, 129 (1979).
19. T. Guillot, D. Gautier, G. Chabrier, B. Mosser, *Icarus* **112**, 37 (1994).
20. K. Rages, J. B. Pollack, M. G. Tomasko, L. R. Doose, *ibid.* **89**, 359 (1991).
21. K. H. Baines and H. B. Hammel, *ibid.* **109**, 20 (1994).
22. P. J. Gierasch and B. J. Conrath, *J. Geophys. Res.* **92**, 15019 (1987).
23. In the troposphere, the abundance of methane is not expected to decrease with increasing pressure. Therefore, a temperature profile retrieved from occultation data assuming no methane in the atmosphere minimizes the temperature gradient at any given altitude. I calculated the lower bound of the filled areas in Fig. 2 under this assumption, using refractivities provided by F. M. Flasar and P. J. Schinder (personal communication) and from (*10*). In order to estimate an upper bound, I assumed an abundance of methane of 60 times the solar value in the interior, and a corresponding relative humidity of ~0.7 in Uranus and ~0.15 in Neptune (calculated so as to explain variations of the refractivity profiles). Larger values of the temperature gradient are possible for more rapid variations of the methane abundance.
24. A. Marten *et al.*, *Astrophys. J.* **406**, 285 (1993); S. Guilloteau, A. Dutrey, A. Marten, D. Gautier, *Astron. Astrophys.* **279**, 661 (1993); K. Lodders and B. Fegley Jr., *Icarus* **112**, 368 (1994).
25. H. B. Hammel *et al.*, *Science* **267**, 1288 (1995).
26. A. P. Ingersoll and H. Kanamori, *Nature* **374**, 706 (1995).
27. The adiabatic gradients shown here assume that ortho- and para-hydrogen are in equilibrium. In Uranus and Neptune, the adiabatic gradient can be substantially larger if ortho-para transitions are not allowed (at 1 bar, $\nabla_{ad}^{normal} \sim 0.4$ compared to $\nabla_{ad}^{eq} \sim 0.28$ for the equilibrium adiabat) [S. T. Massie and D. M. Hunten, *Icarus* **49**, 213 (1982); B. J. Conrath and P. J. Gierash, *ibid.* **57**, 184 (1984)]. Such a gradient is not consistent with the measured temperature profile for $P \lesssim 0.8$ bar in Uranus and $P \lesssim 1$ bar in Neptune. Furthermore, spectroscopic observations show that the ortho and para populations are in equilibrium [K. H. Baines, M. E. Mickelson, L. E. Larson, D. W. Ferguson, *ibid.* **114**, 328 (1995)]. The use of a normal (or intermediate) adiabatic gradient to model microwave spectra of these planets (*13*) relies on the implicit hypothesis that convection occurs and is adiabatic.
28. E. Anders and N. Grevesse, *Geochim. Cosmochim. Acta* **53**, 197 (1989).
29. I gratefully acknowledge discussions with D. Saumon, J. I. Lunine, D. Gautier, W. B. Hubbard, A. P. Ingersoll, and S. Malham. I thank F. M. Flasar and P. J. Schinder for kindly providing me with Neptune's refractivity profile, and two anonymous referees for helpful comments on the manuscript. This research was supported by a fellowship of the European Space Agency and by NSF grant AST-93-18970.

24 April 1995; accepted 26 July 1995

An Improved Procedure for El Niño Forecasting: Implications for Predictability

Dake Chen, Stephen E. Zebiak, Antonio J. Busalacchi, Mark A. Cane

A coupled ocean-atmosphere data assimilation procedure yields improved forecasts of El Niño for the 1980s compared with previous forecasting procedures. As in earlier forecasts with the same model, no oceanic data were used, and only wind information was assimilated. The improvement is attributed to the explicit consideration of air-sea interaction in the initialization. These results suggest that El Niño is more predictable than previously estimated, but that predictability may vary on decadal or longer time scales. This procedure also eliminates the well-known spring barrier to El Niño prediction, which implies that it may not be intrinsic to the real climate system.

Indices of El Niño, such as equatorial Pacific sea-surface temperature (SST) anomalies, can presently be predicted by statistical models several months in advance and by physical coupled ocean-atmosphere models at lead times exceeding 1 year (*1–3*). It is not yet known how much more room there is for improvement in modeling, observation, and forecasting techniques. There is surely a limit to predictability intrinsic to the natural system, a consequence of its chaotic and random nature (*4*). For weather prediction, estimates of this intrinsic limit can be made from models, but we do not have comparable confidence that any of the existing models capture the relevant features of nature's ENSO (El Niño–Southern Oscillation) cycle.

D. Chen, S. E. Zebiak, M. A. Cane, Lamont-Doherty Earth Observatory, Columbia University, Palisades, NY 10964, USA.
A. J. Busalacchi, Laboratory for Hydrospheric Processes, NASA Goddard Space Flight Center, Greenbelt, MD 20771, USA.

One sure bound on intrinsic predictability is the skill of actual predictions. All prior forecast procedures showed a marked drop of skill in forecasts that tried to predict across the boreal spring (*2, 5–8*). The so-called "spring barrier" ("autumn barrier" in the Southern Hemisphere) has been taken as an intrinsic feature of the climate system because, in addition to being common to all forecast models, it appears in auto-correlations of observational indices of ENSO (*9*). The results reported here, however, show only a barely perceptible drop in the skill of springtime forecasts. Previous rather pessimistic theoretical estimates of intrinsic predictability (*5*) must be revised upward to be consistent with the increase in actual skill demonstrated here.

The earliest of the physically based ENSO forecast models is the intermediate coupled model developed by Cane and Zebiak (CZ model) (*1, 6*). The predictive ability of this model has been demonstrated extensively (*1, 2, 10*) but has not been significantly improved since the model was first introduced almost a decade ago. Although this model's predictive skill is most likely limited by its incomplete physics, the overall skill of more complicated coupled general circulation models is not significantly greater at present (*2, 7*).

One possible limitation on many of the forecast systems is the initialization procedure (*1, 2*). Errors in initial conditions are a result of inaccuracies in the observations and deficiencies in the models using the observations. These errors may be reduced by empirically truncating an empirical orthogonal function representation of the data, retaining large-scale, low-frequency signals and discarding small-scale, high-frequency variability or noise (*2, 5, 11–13*). This is a common procedure in hybrid coupled models where an ocean circulation model is coupled to a statistical model of the atmosphere. Alternatively, one may assimilate data into a coupled forecast model. The most common approach is to improve the ocean initial conditions in a stand-alone mode by assimilating observations of SST, thermocline depth, or sea level into an ocean model before coupling with an atmosphere model (*13–16*). The problem with this approach is that no interactions are allowed between the oceanic and atmospheric components during initialization, so the coupled system is not well balanced initially and may experience a shock when the forecast starts. Recently, a coupled approach has also been introduced in which SST and wind data were assimilated into a coupled system for forecast initialization (*15*), but the observations were given such strong weights that the procedure was equivalent to initializing the ocean in a decoupled mode.

We improved the predictive skill of the